

Analysis of flotation and aggregation characteristics of muscovite particles through the extended DLVO theory

Berivan Tunç¹, Onur Guven², Orhan Ozdemir³, Mehmet Sabri Çelik^{1,4}

¹ Istanbul Technical University, Mineral Processing Engineering Department, Istanbul, Turkey

² Adana Alparslan Türkeş Science and Technology University, Mining Engineering Department, Adana, Turkey

³ Istanbul University-Cerrahpaşa, Mining Engineering Department, Istanbul, Turkey

⁴ Harran University, Rectorate, Şanlıurfa, Turkey

Corresponding author: oguvn@atu.edu.tr (Onur Guven)

Abstract: In this study, the flotation and aggregation characteristics of muscovite mineral particles were determined as a function of dodecyl amine hydrochloride (*DAH*) concentration and correlated with the theoretically calculated “particle-particle” and “particle-bubble” interactions using extended *DLVO* theory. In this series of tests, the flotation and aggregation characteristics of the muscovite mineral were determined with micro-flotation and turbidity measurements, respectively. In addition to these analyses, surface tension measurements were carried out as a function of pH. Also, the zeta potential and contact angle measurements were also performed as a function of *DAH* concentration prior to the flotation and aggregation tests. The experimental studies showed that while almost minimum and maximum points of flotation and turbidity values were obtained up to a critical concentration of *DAH* as 6.10^{-6} mol/dm³, a significant increment was obtained following that concentration. Accordingly, while repulsive forces dominated the interactions up to that concentration, the attractive forces became more effective at further concentrations such as 2.10^{-5} , 4.10^{-5} , 8.10^{-5} , and 1.10^{-4} mol/dm³ *DAH* concentrations for both “particle-particle” and “particle-bubble” interactions. This in turn suggested that the determination of energy barrier heights between “particle-particle” and “particle bubble” may provide important insights into both flotation and aggregation characteristics of particles.

Keywords: muscovite, theoretical analysis, particle-particle, particle-bubble, XDLVO, vdW, EDL forces

1. Introduction

Froth flotation is the most widely used and accepted method for separating different minerals based on the adhesion of hydrophobic particles onto bubbles (Pineres et al., 2011). Many publications have focused on explaining this phenomenon by experimental and theoretical assumptions considering particles in either spherical shape, smooth, and completely or partially covered by reagents under predefined conditions (Koh et al., 2009, Verelli et al., 2014; Wang et al., 2014; Drelich and Bowen, 2015; Guven et al., 2015; Guven et al. 2016, Karakas and Hassas, 2016). The results of these previous studies clearly showed that the collector adsorption at the solid/liquid interface was directly related to the wetting characteristics of the sample. For example, a rapid increase was obtained for both flotation and contact angle of quartz upon covering its surface with long-chain alkyl amine at pH range 8-10 (Fuerstenau, 1957), whereas a significant decrease was obtained at pH values over 12.

In another study by Rao et al. 1990, it was found that by the usage of a mixed anionic/cationic collector, the selective flotation of mica minerals such as muscovite and biotite can be achieved with the higher recovery of muscovite from the mixture of muscovite, biotite, and siliceous gangue minerals (feldspar and quartz). Thus, their findings showed that the selection and the dosage of the reagents should be evaluated for the flotation of muscovite. Although many similar studies are present in the literature for the flotation of muscovite, to our knowledge, there is no study to investigate the aggregation characteristics of muscovite under flotation conditions. Therefore, in this study, the same

conditions were adapted to investigate the flotation and aggregation characteristics of muscovite samples.

Besides the experimental approaches, theoretical viewpoints were also used for modeling both bubble-particle and particle-particle interactions that occur during flotation and aggregation processes (Mao, 1998; Liu and Zu, 2007; Guven et al., 2015; Yao et al., 2016; Xing et al., 2017). In this context, the application of classical *DLVO* (Derjaguin-Landau-Verwey-Overbeek) theory has been used for modeling both stabilization and destabilization of charged colloidal particles under different conditions for almost a century (Suresh and Walz, 1996; Gao et al., 2017). In the literature both basic and derivative forms of *DLVO* are used to describe the interactions as the sum of attractive van der Waals and repulsive electrostatic double-layer forces and have been applied to many systems (Suresh and Walz, 1996; Yoon and Mao, 1996; Hoek et al., 2003; Guven et al., 2015; Guven et al., 2022.). However, due to its limitations; it can only be effectively used for low potentials in symmetric electrolyte systems beyond Debye length (Gao et al., 2017). Accordingly, it cannot be used for investigating specific ion effects or in the presence of reagents (Bostrom, 2001). Thus, to address these disagreements, values of other components like hydrophobic (Israelachvili and Adams, 1978; Attard, 1989; Christenson and Claesson, 2001) and hydration forces (Miklavcic, 1995; Grasso et al., 2002) might be considered. These additions then make up the extended *DLVO* (hereafter *XDLVO*) assumption. The total interaction energy curve is usually evaluated to investigate the equilibrium state of colloidal dispersions in the application of this theory (Gao et al., 2017). Therefore, the height of the energy barrier would provide an idea about the stabilized or destabilized conditions of colloidal systems. Similarly, the particle-bubble interactions can also be evaluated in the same manner. Higher barrier heights suggest weaker interactions; lower barrier heights indicate a stronger probability of bubble-particle attachment (Pineres et al. 2011; Güven et al., 2015; Ozdemir et al., 2018).

Therefore, this study aimed to correlate the flotation and aggregation characteristics of a mica mineral "muscovite" with the calculated energy barrier heights against amine concentrations.

2. Materials and methods

2.1. Materials

In this study, mica (muscovite) mineral was received from Kaltun Company (Cine-Milas, Turkey) in lump form (COATTUN-SMW.375 (KM.03. M.0075)). As shown in Table 1, the d_{90} and d_{50} sizes of the sample were determined as 260.0 μm and 50.0 μm , respectively. However, in order to keep the properties of the original sample (directly obtained from the company), both the coarse and fine fractions were screened to obtain -53+38 μm for the experimental studies. The reason for the selection criteria for that size range was to make it suitable for both flotation and aggregation tests. Accordingly, for the calculation of potential energy barriers, the average size of this size range was used as 45.5 μm . The physical properties and chemical analysis of the samples are presented in Tables 1 and 2, respectively.

Table 1. Physical properties of the sample

Particle Size Distribution			Colour			Others				
Malvern Mastersizer 2000			Elrepho 450 TS			Density (g/cm ³)	Bulk Density (g/cm ³)	Mohs Hardness	Humidity (%)	Oil Adsorp (g/100 g)
d_{10} (μm)	d_{50} (μm)	d_{90} (μm)	L^*	a^*	b^*					
12.0	50.0	260.0	92.7	0.2	4	2.85	0.37	2.5	0.3	66

Table 2. Chemical analysis of the sample

Compound	SiO ₂	Al ₂ O ₃	Fe ₂ O ₃	TiO ₂	CaO	MgO	Na ₂ O	K ₂ O	P ₂ O ₅	LOI**
(%)	56.1	27.2	0.98	0.31	0.39	1.55	1.52	8.2	0.25	3.5

* These average values were provided by Kaltun Company sample specification sheets.

** LOI: Loss of ignition

Due to the specifications of this sample for their usage in the paint industry, it requires a high degree of purity to eliminate the possible harmful effects of other components on the quality of paint products. Considering that knowledge in mind, as shown in Tables 1 and 2, the sample can be accepted as sufficiently pure to reveal its characteristics in zeta potential, contact angle, flotation, and aggregation studies. The collector, dodecyl amine hydrochloride (*DAH*) of 98% purity, is a product of Aesar company.

2.2. Methods

2.2.1. Surface tension measurements

A Du Nouy Ring Tensiometer (Krüss®) was used to measure the surface tension of collector solutions at varying concentrations and pH values. The pH value was adjusted with HCl and NaOH aqueous solutions to show the effect of pH value on the surface tension of *DAH* solutions.

2.2.2. Zeta potential measurements

Zeta potential measurements of the sample were carried out as a function of *DAH* concentration using a microprocessor equipped Zeta-Meter 3.0+ model Instrument. All the measurements were carried out under 75 V and the K factor of the measurement cell was 0.71 cm^{-1} . The sample for the zeta potential measurements was prepared as follows: About 0.1 g muscovite sample under $38 \mu\text{m}$ was added to 100 cm^3 collector suspension at desired collector concentration and mixed at 360 rpm for 10 min to provide suitable conditions for the zeta potential measurements. The pH of the medium was adjusted to 9.5 ± 0.02 with $1.10^{-3} \text{ mol/dm}^3$ NaOH addition, and both initial and final pH values of the liquids were recorded for each measurement. The average of at least ten measurements together with their standard deviations for each dispersion was recorded.

2.2.3. Contact angle measurements

The contact angle is an important indicator for determining the wettability degree of mineral surfaces (Kowalcuk et al., 2017). The type of contact angle as dynamic, advancing, and receding plays a crucial role in identifying analysis of different forces occurring during bubble-particle and particle-particle interactions (Drellich et al. 1997; Shang et al., 2008). In addition to the type, different methods of measuring contact angle such as sessile drop, capillary rise, thin layer wicking, and drop shape analysis, i.e., can also provide useful information on these forces (Shang et al., 2008; Ozdemir et al., 2009; Guven et al., 2015). However, the selection criteria for the type of contact angle and measurement technique are simply related to the surface or material's physical characteristics as such differences may be obtained for the same measurements performed on powder and plate type materials (Karaguzel et al., 2005). Contact angle measurements of muscovite surfaces were carried out with the "Sessile Drop" method by OCA15EC model goniometer, SCA 20 software, Data Physics Instruments GmbH, Filderstadt, Germany). The values were recorded in degrees. The measurements were conducted on muscovite plates ($3 \times 3 \text{ cm}$ in size) which were extensively cleaned with alcohol and distilled water (TDS: $14 \mu\text{mhos/cm}$). Before the measurements, the pH of the amine solutions was adjusted to 9.5 ± 0.2 by NaOH to provide the same conditions in flotation and aggregation tests. The muscovite plates were conditioned in these solutions for 1 hour and then dried with nitrogen to ensure the dryness and cleanliness of the surface before the measurements. The same amount of water was dropped onto the muscovite plates in a syringe with a 1 cm^3 volume. At least three measurements were conducted on different locations of the same plate and the averages of measurements were used in energy barrier calculations.

2.2.4. Micro-flotation experiments

Micro-flotation experiments were carried out in a 150 cm^3 micro-flotation column cell with a ceramic frit (pore size of $15 \mu\text{m}$) which was mounted on a magnetic stirrer and a magnetic bar used for agitation. The experiments were carried out with 1 g of $-3+38 \mu\text{m}$ sized samples in the presence of *DAH*. The samples were initially conditioned with the collector solution for 5 min and pH was adjusted to 9.5 with

1.10⁻³ mol/dm³ NaOH to avoid precipitation of amine before the flotation experiments. After the conditioning, the suspension was transferred to the flotation cell and the samples were floated for 1 min by using N₂ gas at a flow rate of 50 cm³/min. The amount of muscovite particles in both float and sink products was gravimetrically measured.

2.2.5. Turbidity measurements

Aggregation tests were carried out under the same conditions with flotation experiments as a collector concentration, pH, and conditioning time to mimic the conditions without a bubble medium. After the conditioning stage, the suspension was transferred to the measurement tube and placed in a turbidity meter (WTW 430 T Model). All analyses were made following the procedure explained in standard ASTM D7315-17. The volume of the measuring tube was 20 cm³ and due to the fast settling rate of particles, the solid wt.% was selected as 0.157% to enable the recording of solution turbidity as a function of time.

2.2.6. Energy barrier analysis

As mentioned in the "Introduction" section, the application of classical DLVO theory generally fails when the surfaces are very hydrophilic or hydrophobic (Yao et al., 2016). Although the long-range repulsive electrical double layer forces dominate most of the systems, in the case of flotation and aggregation studies, the additional components like hydrophobic forces concerning polar interfacial interaction (Yoon and Mao, 1996; Guven et al., 2015) provide a better explanation for the interactions between bubbles and particles. Measuring the stability of an aqueous film and the associated energy barrier that prevents the particle from attachment to a gas bubble can dictate the outcome and rate of flotation processes (Laskowski et al. 1991). Although analysis of the energy barrier height between particles has received considerable popularity, little attention was given, however, to understanding and quantification of the energy barrier for particle-bubble interactions (Ozdemir et al., 2018).

Therefore, in this study, besides classical DLVO interactions such as van der Waals and electrostatic double-layer forces (Suresh and Walz, 1996), hydrophobic forces were also incorporated in theoretical calculations to provide a better explanation and correlation with flotation recoveries. Thus, considering the plate shape structure of mica particles and the spherical shape structure of bubbles, the equations for plate-sphere geometry were used for the energy barrier calculations between particle-particle and bubble-particle. Although the radius of bubbles would change upon increasing amine concentration in the system (Corona-Arroyo et al., 2015) the same radius values were used in these calculations since no experimental data is present for bubble size variation. Additionally, the Debye length value would also change under the same conditions but since no adsorption data is present for the presence of amine in the solution, the Debye length was taken constantly through all calculations. The calculation of the Van der Waals force is given in Eq. 1:

$$E_{vdW} = 2\pi RA \left[\frac{-2.45\lambda}{120\pi^2 h^2} + \frac{2.17\lambda^2}{720\pi^3 h^3} - \frac{0.59\lambda^3}{3360\pi^4 h^4} \right] \quad (1)$$

where A is the Hamaker constant, R is the radius of the particle (μm), λ is the characteristic wavelength, and " h " is the separation distance (nm) as measured from the mineral particle surface. The equation describing the electrical double layer forces is given below as Eq. 2:

$$E_{EDL-SS} = 16R(4\pi\epsilon\epsilon_0) \left(\frac{kT}{e} \right)^2 \tanh\left(\frac{e\psi_1}{4kT}\right) \tanh\left(\frac{e\psi_2}{4kT}\right) e^{-\kappa h} \quad (2)$$

where ψ_1 and ψ_2 are the surface potentials of particle and gas bubbles respectively, k is the Boltzmann constant ($1.38 \times 10^{-23} \text{ m}^2\text{kg}\cdot\text{s}^{-2}\text{K}^{-1}$), and e is the charge of a proton ($1.602 \times 10^{-19} \text{ C}$), T is the temperature (298 K), κ^{-1} is the Debye length, ϵ is the bulk dielectric constant (80), ϵ_0 is the permittivity of free space ($8.85 \times 10^{-12} \text{ C}^2\text{J}^{-1}\text{m}^{-1}$). For the calculation of hydrophobic forces, a similar equation derived from the Hamaker approach was used as Eq. 3:

$$V_{hydrophobic} = -\frac{K_H R}{12h} \quad (3)$$

Unlike A_H in vdW forces, K_H represents the hydrophobic constant between bubble and particle which can be calculated using Eq. 4.

$$K_H = ae^{b\kappa\theta} \quad (4)$$

where a and b_K are constants that vary with contact angle (Pazhianur and Yoon, 2003; Ozdemir et al., 2018).

3. Results and discussion

3.1. Surface tension measurements

Surface tension, a measure of surfactant activity, was determined with a series of tests conducted at different pH and concentrations. Long-chain amine-type cationic surfactants generally exhibit a minimum surface tension at a pH where ion molecular complexes form. This pH value corresponds to 9.52. It is worth noting that above and below this pH value, the surface tension values sharply increase in the range of about 8 to 11 (Fig. 1). These findings are in line with the previously reported literature (Yoon and Ravishankar, 1996; Wang and Miller, 2018). For example, Yoon and Ravishankar (1996) conducted direct force measurement with mica surface in dodecyl amine solution at alkaline pH and found that long-range hydrophobic forces were observed at pH 9.5 which is due to co-adsorption of dodecyl ammonium ions and dodecyl amine on the mica surfaces; this is in agreement with our findings for surface tension measurements.

Additionally, it can be seen from Fig. 1 that while a negligible variation was obtained at $\text{pH} < 9$, a considerable variation was obtained when the pH value was adjusted to 9-9.5 independent of concentration.

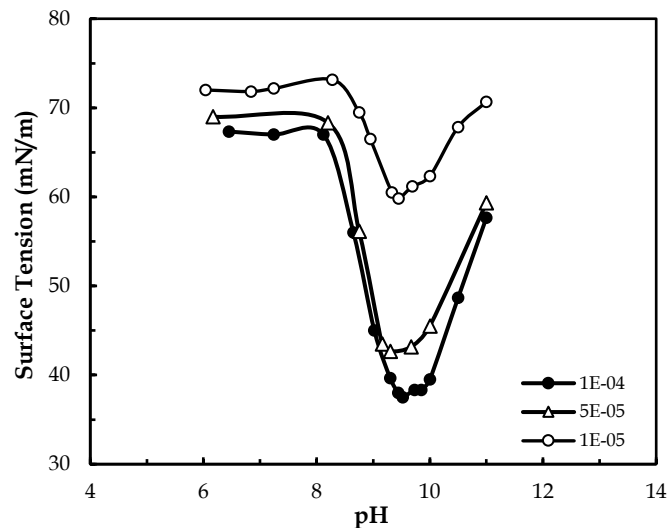


Fig. 1. Surface tension values of DAH as a function of pH

These findings were also in line with the floatability of muscovite minerals which will be further discussed in terms of energy barrier height in the following sections.

3.2. Zeta potential measurements

Mica minerals generally exhibit negatively charged basal planes and edges accounting for 5-10% of the overall surface charge resulting in a net mineral iso-electric point (*iep*) in the range of 4-7.5 (Nosrati et al., 2012; Xu et al. 2013; Yan et al. 2013). Based on the charge distribution over pH and adsorption mechanisms of reagents on mica surfaces, cationic collectors are generally preferred over anionic collectors in the flotation of mica minerals (Rai et al. 2011; Marion et al. 2015). Furthermore, amines are generally adsorbed on mineral surfaces through electrostatic attraction, and thus increase the pH above the solubility of amine at around pH: 9.6; this is found beneficial whereas, above the point of hydrolysis, flotation sharply decreases (Yoon and Ravishankar, 1996; Xu et al. 2013).

Variation of zeta potential against pH provides useful knowledge about possible interactions of particles in flotation and aggregation systems and also helps identify the type and level of interactions between particles. Zeta potential measurements were thus carried out as a function of DAH concentration at $\text{pH } 9.3 \pm 0.2$. As shown in Fig. 2, while the negative values were measured at low

concentrations such as -48.8 mV at 1.10^{-6} mol/dm³, a sudden increase to -36.4 mV was obtained at 2.10^{-5} mol/dm³. And, at higher concentrations, a considerable increase in positive values was obtained. This trend of muscovite is in line with those measured by Rao et al. (1995).

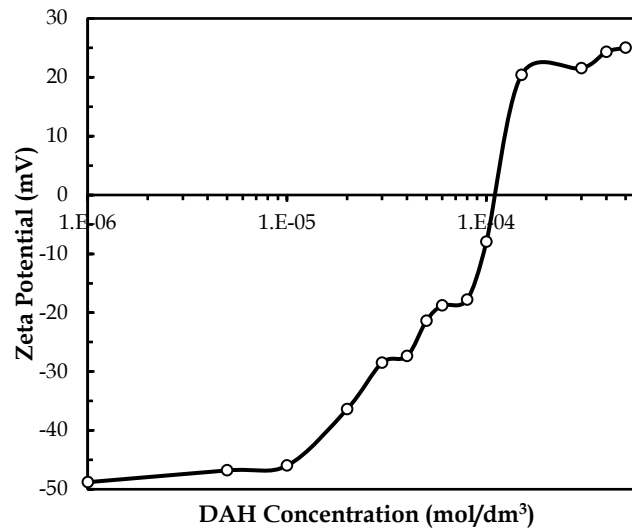


Fig. 2. Zeta potential values of muscovite as a function of *DAH* concentration under constant pH 9.3 ± 0.2

3.3. Contact angle measurements

In this study, the sessile drop method was used for the contact angle measurements. For these tests, muscovite sheets were conditioned under the same conditions as in micro-flotation experiments at pH 9.3. The sheets were conditioned and dried under N₂ gas. The results are shown in Table 3. The results are in close agreement with the previous contact angle measurements carried out by Pugh et al. (1996). Although very close values were obtained as a function of amine concentration that was reported in a recent publication by Wang et al. (2018), the authors also investigated the effect of alcohol usage in the presence of dodecyl amine (DDA) at different ratios which were found to be effective on increasing the contact angle values and hydrophobicity.

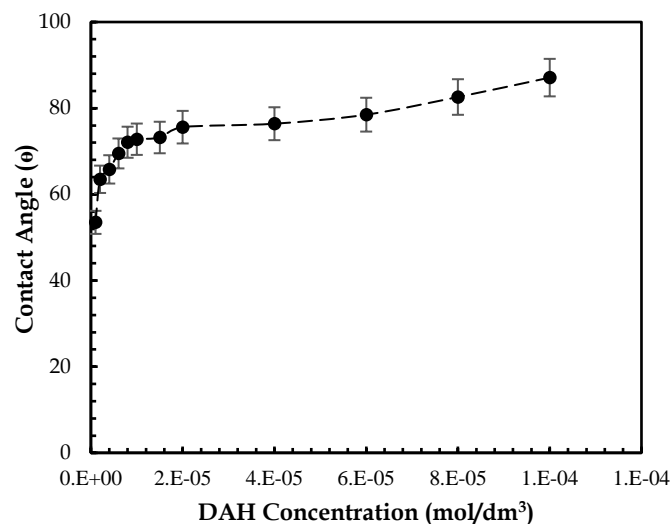


Fig 3. Contact angle measurements as a function of *DAH* concentration

3.4. Micro-flotation experiments and aggregation tests

In this series of tests, micro-flotation and aggregation tests were carried out at different amine concentrations, and the results are shown in Fig. 4.

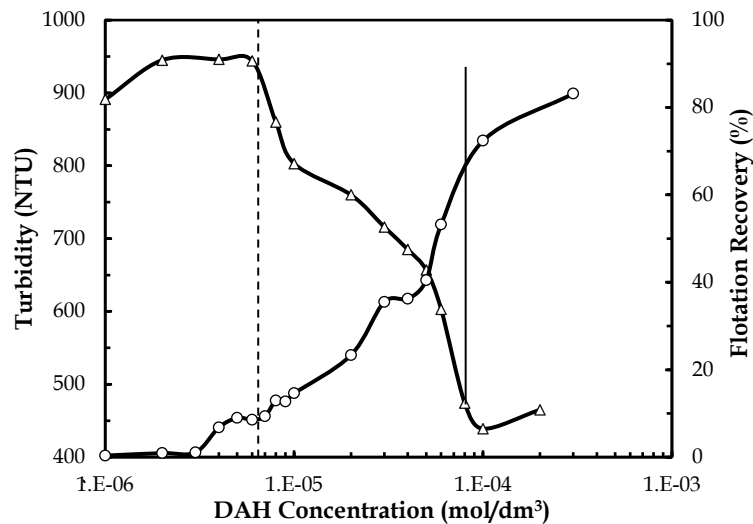


Fig. 4. Flotation and aggregation behavior of muscovite with *DAH*

As seen from Fig. 4, both flotation and aggregation behaviour of muscovite particles followed a reverse trend upon increasing the collector concentration. In other words, while the turbidity values in the no flotation zone were found almost the same in the range of 940-950 NTU until 6.10^{-4} mol/dm³ *DAH*, a considerable decrease was obtained with increasing *DAH* concentrations. This is interesting as it exemplifies the anticipated but not much-proven relationship of the concurrent aggregation trend of particles at the onset of flotation. The aggregation results can be ascribed to the distribution of the adsorbed light emission. At lower concentrations of *DAH* such as 5.10^{-5} mol/dm³ and 4.10^{-5} mol/dm³, very close values were obtained for both flotation and aggregation rates. In other words, while the flotation recovery values were 36.2% and 40.5% for these concentrations, the aggregation tendencies rates were measured as 685 and 657 NTU. However, at 6.10^{-5} mol/dm³ *DAH*, while the flotation recovery increased to 53.2%, the aggregation rate decreased to 603 NTU. From these results, it is apparent that both bubble-particle and particle-particle interactions become stronger after the breakthrough point.

3.5. Energy barrier calculations

In this study, the energy barrier between muscovite particles conditioned at certain concentrations of *DAH* and also particle-bubble interactions under the same conditions was theoretically demonstrated and evaluated with the experimental results. Furthermore, a comparison was made between the calculated energy barrier heights between particle-particle and particle-bubble which could explain the contribution of hydrophobic force generated by the hydrophobic nature of bubbles in amine solutions.

The total interaction potential energy is shown for five *DAH* concentrations ranging from 1.10^{-5} to 1.10^{-4} mol/dm³ for both particle-particle (P-P) and particle-bubble (P-B); the following parameters were used: (i) van der Waals interactions ($A = 5.35 \times 10^{-21}$ J, $\lambda = 30$ nm); (ii) electrical double layer interactions, zeta potentials of particles were taken from Fig. 1, while the charge of the bubbles was interpolated from the values reported in the literature (Laskowski et al. 1989), $\kappa^{-1} = 9.6$ nm.

As shown in Fig. 5a, the total interaction energy follows the same trend as Electrical Double layer (EDL) interactions at very low *DAH* concentrations at 1.10^{-6} mol/dm³ whereas the hydrophobic interactions between particles were found to be weak as vdW interactions. From this output, it can be concluded that the repulsive forces mainly dominate the interactions between particles at low *DAH* concentrations. However, the contribution of hydrophobic forces in Fig. 5b clearly showed an increasing trend at higher *DAH* concentrations. Therefore, unlike weak vdW forces, attractive forces appear at higher separation distances upon the contribution of hydrophobic interactions which in turn affects the wettability characteristics of particles (Guven et al., 2015). As a result, the total interaction energy decreased towards lower heights and resulted in more attractive interaction between particles which is then reflected in lower turbidity values seen in Fig 4.

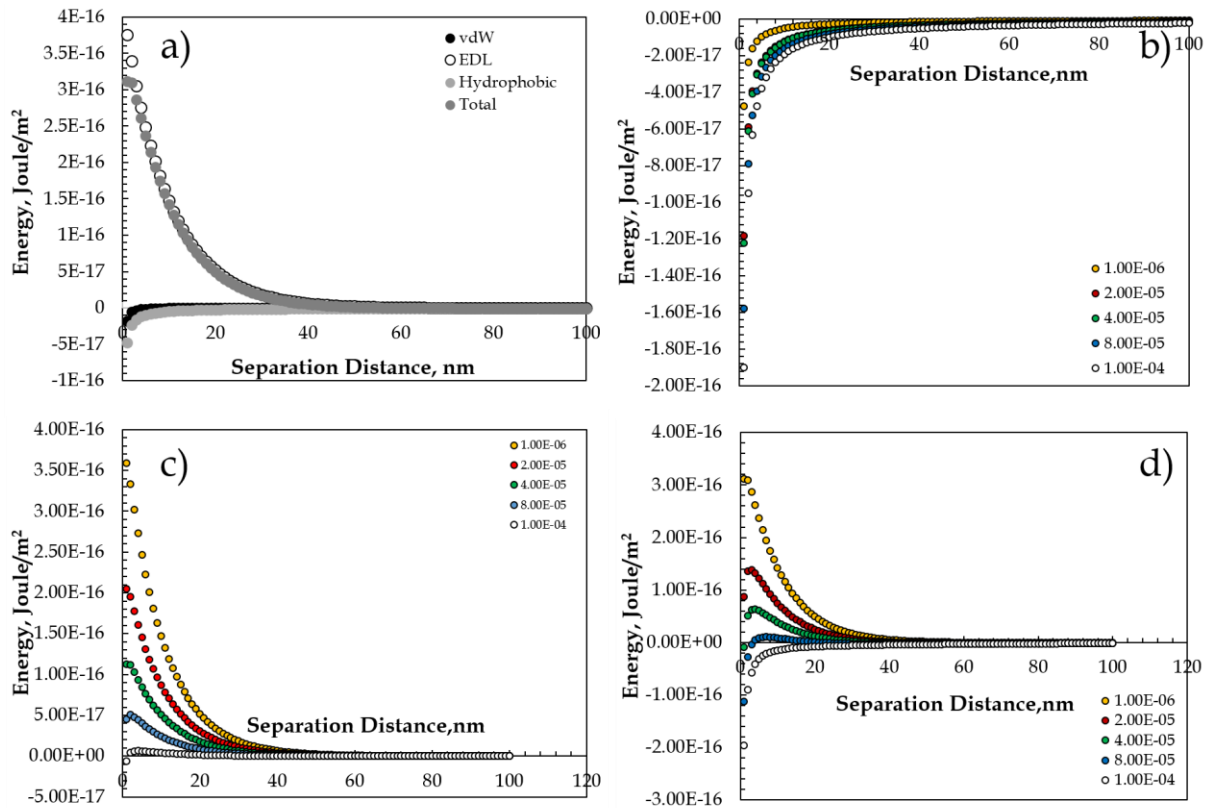


Fig. 5. a) vdW, EDL, and Hydrophobic interactions for 1.10^{-6} mol/dm³ DAH. b) Hydrophobic interactions as a function of DAH concentration. b) Total energy calculations without hydrophobic interaction between muscovite particles. b) Total energy calculations with hydrophobic interaction between muscovite particles

The role of hydrophobic interactions on total energy calculations between particles is further exemplified separately in two graphs (with and without the presence of hydrophobic interactions) in Figs. 5c and 5d. In Fig. 5c (without the presence of hydrophobic interaction), the maximum and minimum energy barrier heights were calculated as 3.59×10^{-16} J/m² and 5.36×10^{-17} J/m² for 1.10^{-6} mol/dm³ and 1.10^{-4} mol/dm³ DAH concentrations. These values also indicated the weakness of vdW interactions alone for explaining the attractive interactions between particles. In other words, very close values were obtained for energy barrier height values even at higher concentrations (Pazhianur and Yoon, 2003). As mentioned above, considerable differences in aggregation abilities between particles were obtained upon increasing DAH concentrations which then demonstrated the need for accounting for hydrophobic interactions to explain the theoretical explanations of experimental findings.

Taking into account hydrophobic interactions, lower energy barrier height values were obtained as 3.10×10^{-16} J/m² and 4.07×10^{-18} J/m² for 1.10^{-6} mol/dm³ and 1.10^{-4} mol/dm³ DAH concentrations. These findings are in line with the aggregation characteristics of muscovite particles in terms of turbidity values shown in Fig. 4.

Particle-particle interactions and the total interaction energies between bubbles and muscovite particles were calculated and presented in Fig. 6. Although some variations in bubble diameters are known to occur at different DAH concentrations (Corona-Arroyo et al., 2015) in terms of Sauter mean diameter (mm), it was shown that while at a DAH concentration of 1.0 mg/dm³, the bubble size was measured as 3.6 ± 0.1 mm, it gradually decreased to 0.7 ± 0.1 mm at DAH concentration of 8.0 mg/dm³. However, to better evaluate the energy barrier values for bubble-particle interactions, the bubble diameter was assumed the same as the particle diameter. Apart from the previous ones, the surface charge of bubbles ψ_B , in these calculations was taken constantly as -25 mV (Elmahdy et al., 2008). Thus, if a comparison was made between the particle-particle interactions (Fig 5d) and bubble-particle interactions, a considerable difference can be seen against DAH concentrations shown in Fig. 6. In other words, while the energy barrier was 1.57×10^{-16} J/m² for bubble-particle interactions, it was found as 3.59×10^{-16} J/m²

for particle-particle interactions at a *DAH* concentration of 1.0×10^{-6} mol/dm³. A similar trend was also obtained for higher concentrations of *DAH*. Accordingly, while the energy barrier was 2.30×10^{-17} J/m² for bubble-particle interactions, it was found as 6.86×10^{-17} J/m² for particle-particle interactions at *DAH* concentration of 8×10^{-5} mol/dm³. At this point, it is worth noting that the presence of a bubble in the system decreased the energy barrier almost threefold which is proportional to the flotation results under the same conditions.

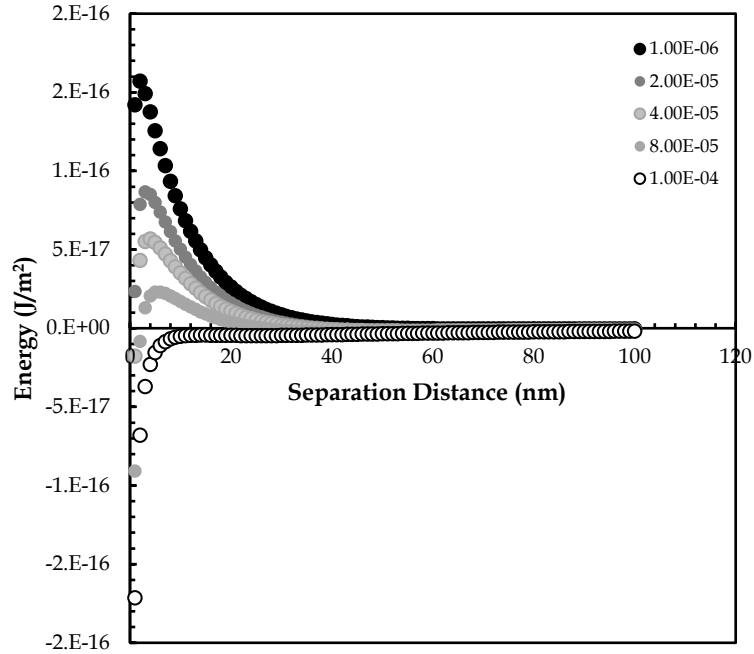


Fig. 6. Total energy calculations including hydrophobic interaction between the single bubble and muscovite particles

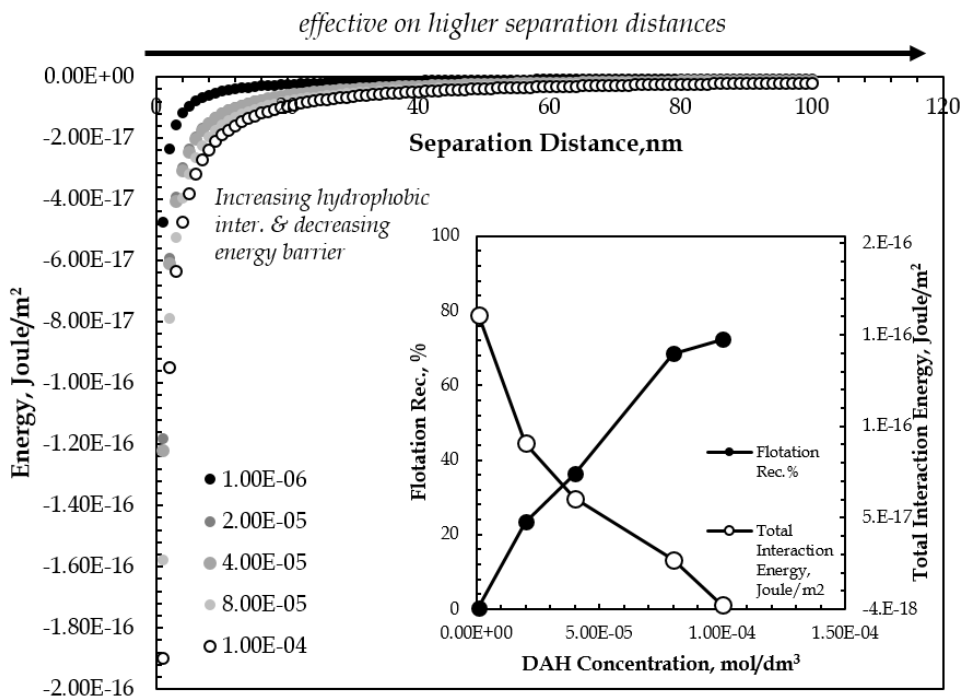


Fig. 7. Illustration of hydrophobic interactions for bubble-particle interactions and the total interaction energy vs. flotation recovery values (inset Fig.) against *DAH* concentration

Fig. 7 shows the contribution of hydrophobic forces to particle-bubble interactions. The negative trend in the energy barrier values between particle and bubble resulted in higher flotation recoveries. The graph in Fig. 7 shows that upon introducing the hydrophobic interactions, the attractive interactions became effective even at higher separation distances which then proportionally changed the trend of total interactions to more attractive values. In this manner, plotting the total energy barrier (inset Fig.) vs flotation recovery values proved that lower total interaction energies resulted in attractive bubble-particle interactions. In other words, aggregation is a prerequisite for improved flotation recoveries. As shown in Fig. 4, while a negligible amount of muscovite can be floated (0.3%) at low concentrations of 1.10^{-6} mol/dm³, it increased to 72.4% at a higher concentration of 1.10^{-4} mol/dm³. The energy barrier values at the same concentrations were correspondingly varied from 1.57×10^{-16} J/m² to 1.90×10^{-18} J/m² which in turn showed that the energy barrier height values are directly proportional to the flotation of muscovite particles.

Similar findings were also reported by Mao et al. (1998) in which the increasing the methylation degree of glass beads resulted in more attractive interactions between bubble and particle consequently resulting in higher flotation kinetics. Also, Pugh et al. (1996) calculated force normalized by radius as a function of separation between mica immersed in an aqueous solution of 1.10^{-4} mol/dm³ DAH solution and disclosed that an attractive deviation from DLVO theory can be observed at separations below 15 nm which is in relative agreement with the results presented in Figs. 5 and 6.

4. Conclusions

In this study, the extended-DLVO theory was examined for flotation and aggregation of muscovite particles in the presence of dodecyl amine hydrochloride (DAH). The zeta potential measurements, micro-flotation experiments, and aggregation studies were performed in a pH range of 9-9.5. The results obtained from this study indicate that there is a good correlation between flotation and turbidity of muscovite particles as a function of DAH concentration. It is seen that at a threshold DAH concentration of 6.10^{-6} mol/dm³ a sharp increase in flotation recovery and a decrease in turbidity values were obtained. At this concentration, the correlation of theoretical energy barriers and experimental results indicated that the attractive forces between muscovite particles dominated the attractive interactions above the 6.10^{-6} mol/dm³ DAH concentration and shifted the attractive components in favour of hydrophobic forces to higher separation distances from 0 to 23 nm. The presence of hydrophobic forces competed with the repulsive forces in the system and induced aggregation of particles to enhance the flotation of mica particles. In this manner, while a high energy barrier such as 1.57×10^{-16} J/m² was obtained for 1×10^{-6} mol/dm³ DAH concentration, it decreased to 2.30×10^{-17} J/m² at 8×10^{-5} mol/dm³. Finally, the theoretical energy barrier height values were found in line with the experimental results and can be used to predict the flotation and aggregation characteristics of muscovite particles. In the light of these findings, the effects of other parameters such as type of mica and reagents can also be investigated in terms of their flotation and aggregation characteristics with the help of both experimental and theoretical findings.

Acknowledgments

This study is supported by The Scientific and Technological Research Council of Turkey (TUBITAK) with project number 117M659. The authors also would like to express their gratitude to Prof. Dr. Mehmet Sabri Çelik for his kind motivation and guidance throughout their academic life.

References

- ASTM D7315-17. 2018. *Standard Test Method for Determination of Turbidity Above 1 Turbidity Unit (TU) in Static Mode*. ASTM International.
- ATTARD, P., 1989. *Long-range attraction between hydrophobic surfaces*. J. Phys. Chem., 93, 6441-6444.
- BOSTROM, M. WILLIAMS, D.R.M., NINHAM, B.W., 2001. *Specific ion effects: Why DLVO theory fails for biology and colloid systems*. Physical Review Letters, 87, 16, 1-4.
- CHRISTENSON, H.K. and CLAEISSON, P.M., 2001. *Direct measurements of the force between hydrophobic surfaces in water*. Advances in Colloid and Interface Science, 91, 391-436.

- CORONA-ARROYO, M.A., LOPEZ-VALDIVIESO, A., LASKOWSKI, J.S., ENCINAS-OROPESA, A., 2015. *Effect of frothers and dodecylamine on bubble size and gas holdup in a downflow column*. Minerals Engineering, 81,109-115.
- DRELICH, J., 1997. *The effect of drop (bubble) size on contact angle at solid surfaces*. The Journal of Adhesion, 63, 1-3, 31-51.
- DRELICH, J. and BOWEN, P.K., 2015. *Hydrophobic nano-asperities in control of energy barrier during particle-surface interactions*. Surface Innovations, 3(3), 164-171.
- ELMAHDY, A.M., MIRNEZAMI, M., FINCH, J., 2008. *Zeta potential of air bubbles in presence of frothers*. International Journal of Mineral Processing, 89(1-4), 40-43.
- FUERSTENAU, D.W., 1957. *Correlation of contact angle, adsorption density, zeta potentials and flotation rate*. AIME Transactions, 208, 1365-1367.
- GAO, Y., EVANS, G.M., WANLESS, E.J., MORENO-ATANASIO, R., 2017. *DEM modelling of particle-bubble capture through extended DLVO theory*. Colloids and Surfaces A, 529, 876-885.
- GUVEN, O., CELIK, M.S., DRELICH, J.W., 2015. *Flotation of methylated roughened glass particles and analysis of particle-bubble energy barrier*. Minerals Engineering, 79, 125-132.
- GUVEN, O., CELIK, M.S., 2016. *Interplay of particle shape and surface roughness to reach maximum flotation efficiencies depending on collector concentration*. Mineral Processing and Extractive Metallurgy Review, 37, 412-417.
- GUVEN, O., KAYMAKOGLU, B., EHSANI, A., HASSANZADEH, A., SIVRIKAYA, O., 2022. *Effects of grinding time on morphology and collectorless flotation of coal particles*. Powder Technology, 399, 117010.
- GRASSO, D., SUBRAMANIAM, K., BUTKUS, M., STREVETT, K., BERGENDAHL, J., 2002. *A review of non-DLVO interactions in environmental colloidal systems*. Re/Views in Environmental Science & Bio/Technology, 1, 17-38.
- HOEK, E.M.V., BHATTACHARJEE, S., ELIMELECH, M., 2003. *Effect of membrane surface roughness on colloid-membrane DLVO interactions*. Langmuir, 19, 4836-4847.
- ISRAELACHVILI, J.N. and ADAMS, G.E., 1978. *Measurement of forces between two mica surfaces in aqueous electrolyte solutions in the range 0–100 nm*. Journal of the Chemical Society, Faraday Trans, 74, 975–1001.
- KARAGUZEL, C., CAN, M.F., SONMEZ, E., CELIK, M.S., 2005. *Effect of electrolyte on surface free energy components of feldspar minerals using thin-layer wicking method*, Journal of Colloid and Interface Science, 285,1, 192-200.
- KARAKAS, F. and HASSAS, B.V., 2016. *Effect of surface roughness on interaction of particles in flotation*. Physicochemical Problems of Mineral Processing, 52 (1), 19-35.
- KOH, P.T.L., HAO, F.P., SMITH, L.K., CHAU, T.T., BRUCKARD, W.J., 2009. *The effect of particle shape and hydrophobicity in flotation*. International Journal of Mineral Processing, 93, 128-134.
- KOWALCZUK, P.B., AKKAYA, C., ERGUN, M., JANICKI, M.J., SAHBAZ, O., DRZYMALA, J., 2017. *Water contact angle on corresponding surfaces of freshly fractured fluorite, calcite and mica*. Physicochemical Problems of Mineral Processing, 53, 1, 192-201.
- LASKOWSKI, J.S., XU, Z., YOON, R.H., 1991. *Energy barrier in particle-to-bubble attachment and its effect on flotation kinetics*. In: Paper read at XVIIth International Mineral Processing Congress, at Dresden, Germany, September 23–28.
- LASKOWSKI, J.S., YORDAN, J.L., YOON, R.H., 1989. *Electrokinetic potential of microbubbles generated in aqueous solutions of weak electrolyte type surfactants*. Langmuir, 5, 373-376.
- LIU, J. and XU, Z., 2007. *Role of flotation reagents in tuning colloidal forces for sphalerite-silica separation*. Canadian Metallurgical Quarterly, 46 (3) 329-340.
- MAO, L. 1998. *Application of extended DLVO theory: Modelling of flotation and hydrophobicity of dodecane*. Ph.D. Thesis, Virginia Polytechnic Institute and State University.
- MARION, C., JORDENS, A., MCCARTHY, S., GRAMMATIKOPOULOS, T., 2015. *An investigation into the flotation of muscovite with an amine collector and calcium lignin sulfonate depressant*. Separation and Purification Technology, 149, 216-227.
- MIKLAVCIC, S.J., 1995. *Double layer forces between heterogeneous charged surfaces: The effect of net surface charge*. The Journal of Chemical Physics, 103, 11, 4794-4806.
- NOSRATI, A., ADDAI-MENSAH, J., SKINNER, W., 2012. *Muscovite clay mineral particle interactions in aqueous media*. Powder Technology, 219, 228–238.
- OZDEMIR, O., KARAGUZEL, C., NGUYEN, A.V., CELIK, M.S., and MILLER, J.D., 2009. *Contact angle and bubble attachment studies in the flotation of trona and other soluble carbonate salts*. Minerals Engineering, 22(2), 168-175.

- OZDEMIR, O., ERSOY, O.F., GUVEN, O. TURGUT, H. CINAR, M., CELIK, M.S., 2018. *Improved flotation of heat treated lignite with saline solutions containing mono and multivalent ions*. *Physicochemical Problems of Mineral Processing*, 54,4, 1070-1082.
- PAZHIANUR, R. and YOON, R.H., 2003. *Model for the origin of hydrophobic force*. *Minerals and Metallurgical Processing*, 20(4), 178-184.
- PINERES, J. and BARRAZA, J., 2011. *Energy barrier of aggregates coal particle-bubble through the extended DLVO theory*. *International Journal of Mineral Processing*, 100, 14-20.
- PUGH, R.J., RUTLAND, M.W., MANEV, E., CLAEISSON, P.M., 1996. *Dodecylamine collector – pH effect on mica flotation and correlation with thin aqueous foam film and surface force measurements*. *International Journal of Mineral Processing*, 46, 245–262.
- RAI, B., SATHISH, TANWAR, P.J., PRADIP, K.S. MOON, FUERSTENAU, D.W., 2011. *A molecular dynamics study of the interaction of oleate and dodecylammonium chloride surfactants with complex aluminosilicate minerals*. *Journal of Colloid and Interface Science*, 362, 510–516.
- RAO, K.H., ANTTI, B.-M., FORSBERGG, K.S.E., 1990. *Flotation of mica minerals and selectivity between muscovite and biotite while using mixed anionic/cationic collectors*. *Mining Met. Explor.*, 7, 127-132.
- RAO, K.-H., CASES, J.M., BARRES, O., FORSBERG, K.S.E., 1995. *Flotation, electrokinetic and FT-IR studies of mixed anionic/cationic collectors in muscovite-biotite system*. *Mineral Processing: Recent Advances and Future Trends*, 29-44.
- SHANG, J., FLURY, M., HARSH, J.B., ZOLLARS, R.L., 2008. *Comparison of different methods to measure contact angle of soil colloids*. *Journal of Colloid and Interface Science*, 328, 299-307.
- SURESH, L., WALZ, J.Y., 1996. *Effect of surface roughness on the interaction energy between a colloidal sphere and a flat plate*. *Journal of Colloid and Interface Science*, 183(1), 199-213.
- VERELLI, D.I., BRUCKARD, W.J., KOH, P.T.L., SCHWARZ, M.P., FOLLINK, B., 2014. *Particle shape effects in flotation. Part 1: Microscale experimental observations*. *Minerals Engineering*, 58, 80–89.
- WANG, L., SUN, W., HU, Y.H., XU, L.H., 2014. *Adsorption mechanism of mixed anionic/cationic collectors in muscovite-quartz flotation system*. *Minerals Engineering*, 64, 44–50.
- WANG, X. and MILLER, J., 2018. *Dodecyl amine adsorption at different interfaces during bubble attachment/detachment at a silica surface*. *Physicochem. Probl. Miner. Process.*, 54(1), 81-88.
- WANG, L., SUN, N., LIU, J. TANG, H., LIU, R., HAN, H., SUN, W., HU, Y., 2018. *Effect of chain length compatibility of alcohols on muscovite flotation by dodecyl amine*. *Minerals*, 8(4), 168.
- XING, Y., GUI, X. KARAKAS, F., CAO, Y., 2017. *Role of collectors and depressants in mineral flotation: A theoretical analysis based on extended DLVO theory*. *Minerals*, 7, 223.
- XU, L. WU, H., DONG, F., WANG, L., WANG, Z., XIAO, J., 2013. *Flotation and adsorption of mixed cationic/anionic collectors on muscovite mica*. *Minerals Engineering*, 41, 41–45.
- YAN, L.J., MASLIYAH, J.H., XU, Z.H., 2013. *Interaction of divalent cations with basal planes and edge surfaces of phyllosilicate minerals: Muscovite and talc*. *Journal of Colloid and Interface Science*, 404, 183–191.
- YAO, J., HAN, H., HOU, Y., GONG, E. and YIN, W., 2016. *A method of calculating the interaction energy between particles in minerals flotation*. *Mathematical Problems in Engineering*, Hindawi Press, 1-13.
- YOON, R.H. RAVISHANKAR, S.A., 1996. *Long-range hydrophobic forces between mica surfaces in alkaline dodecyl ammonium chloride solutions*. *Journal of Colloid and Interface Science*, 179, 403–411.
- YOON, R.H., MAO, L.Q., 1996. *Application of extended DLVO theory. 4. Derivation of flotation rate equation from first principles*. *Journal of Colloid and Interface Science*, 181(2), 613– 626.